Scripta Materialia 143 (2018) 10–14

Contents lists available at ScienceDirect

Scripta Materialia

journal homepage: www.elsevier.com/locate/scriptamat

Regular article

Indentation size effect for spherical nanoindentation on nanoporous gold

Young-Cheon Kim [a,1,2], Eun-Ji Gwak [a,1], Seung-min Ahn [a], Na-Ri Kang [a], Heung Nam Han [b], Jae-il Jang [c], Ju-Young Kim [a,d,*]

[a] School of Materials Science and Engineering, UNIST (Ulsan National Institute of Science and Technology), Ulsan 44919, Republic of Korea
[b] Department of Materials Science and Engineering, Seoul National University, Seoul 08826, Republic of Korea
[c] Division of Materials Science and Engineering, Hanyang University, Seoul 04763, Republic of Korea
[d] KIST-UNIST Ulsan Center for Convergent Materials, UNIST, Ulsan 44919, Republic of Korea

ARTICLE INFO

Article history:
Received 25 July 2017
Received in revised form 3 September 2017
Accepted 3 September 2017
Available online xxxx

Keywords:
Nanoporous gold
Nanoindentation
Porous materials
Hardness
Indentation size effect

ABSTRACT

We find that the indentation size effect (ISE) occurs during spherical indentation on nanoporous gold (np-Au). The hardness increases as the indenter radius decreases at a fixed representative strain. We prepare np-Au samples with a ligament size of 26 nm by free-corrosion dealloying and perform multiple spherical nanoindentations with nominal indenter radii of 4, 12, and 50 μm. A nanomechanics model for the ISE during spherical indentation is developed, and the model accurately describes the hardness depending on the indenter radius. We also correlate the ISE trends of spherical and Berkovich indentations along with their differences in terms of the representative strain and the indentation work.

Spherical indentation has been widely studied because unlike geometrically self-similar sharp indenters, spherical indenters introduce various stress–strain fields depending on the indentation depth. Kim et al. [1] proposed a representative stress–strain method using spherical indentation to determine the tensile properties of metals with Hollomon-type strain-hardening behavior. They used the actual contact depth while considering plastic pile-up, derived a representative stress using Tabor's approach [2] by introducing a plastic constraint factor, and optimized the representative strain using a tangent function of the contact angle between the spherical indenter and the sample surface. Pathak and Kalidindi [3] correlated the indentation stress to the indentation strain and the mean pressure on the projected area to the ratio of the contact radius to the indenter radius (a/R). They investigated the effects of experimental conditions such as continuous stiffness measurement (CSM), pop-in events, indenter size, and polishing on the evaluated indentation stress and strain. They also introduced orientation imaging microscopy and Raman spectroscopy combined with spherical indentations to analyze changes in the microstructure of indents. Swadener et al. [4] found that the indentation size effect (ISE) for spherical indentation depended on the indenter radius and not on the indentation depth as in the case of sharp indentation. This indicates that the ISE for the spherical indenter radius must be considered when spherical nanoindentation is carried out at small scales. To explain the ISE for spherical indentation, geometrically necessary dislocations (GNDs) were assumed to form to accommodate the spherical indent. They developed the following spherical ISE model based on the Nix–Gao model [5]:

$$\frac{H}{H_0} = \sqrt{1 + \frac{R^*}{R_p}}, \tag{1}$$

where H and H_0 are the hardness and the macroscopic hardness, respectively; R^* is the characteristic constant for the spherical ISE; and R_p is the indent radius after spherical indentation. This equation could successfully describe the trends in spherical indentation hardness for annealed iridium and oxygen-free copper samples. Spary et al. [6] performed finite element simulations on materials with different yield strengths to show that the ISE for spherical indentation is related to dislocation generation rather than to dislocation interaction.

Nanoporous gold (np-Au) has recently attracted interest because of its outstanding chemical and physical characteristics, easy fabrication and applications [7–16]. Most investigations on the mechanical behavior of np-Au have been conducted using nanoindentation [17–23] for convenience in sample preparation and experiment execution, considering that np-Au is brittle unlike solid gold. One such finding established by employing nanoindentation is that the strength or hardness of np-Au

* Corresponding author at: School of Materials Science and Engineering, UNIST (Ulsan National Institute of Science and Technology), Ulsan 44919, Republic of Korea.
E-mail address: juyoung@unist.ac.kr (J.-Y. Kim).
[1] These authors contributed to this work equally.
[2] Present address: System Convergence Technology Division, Mechanical Safety Technology Center, Korea Testing Laboratory, Jinju-si 52852, Republic of Korea.

http://dx.doi.org/10.1016/j.scriptamat.2017.09.002
1359-6462/

is strongly dependent on the relative density and the ligament size; this finding is in line with the "smaller is stronger" phenomenon observed in gold nanopillars [24,25]. For np-Au, the hardness has been reported to increase as the indentation depth decreases when using a Berkovich indenter [20,26]. Recently, the present authors suggested an ISE model for np-Au when using a sharp indenter [27]. The ISE model for np-Au is an inverse function of the indentation depth; the function is derived by assuming that the indentation work is consumed in the plastic collapse of np-Au caused by compressive and shear forces. Spherical nanoindentations have been carried out to investigate mechanical behavior of np-Au [26]. As mentioned above, spherical indentations provide hardness for various representative strains. However, it has not been studied the ISE behavior in spherical indentation depending on indenter radius, *R*. It is important to understand ISE behavior in spherical indentation when measuring macroscopic hardness of np-Au by using spherical indenter.

Here, we investigate the ISE for spherical indentation on np-Au. To exclude the effect of the ligament size and relative density of np-Au on spherical nanoindentation, np-Au samples with a single ligament size of 26 nm are fabricated using the free-corrosion dealloying process. Nanoindentations are performed on the np-Au samples using three spherical indenters with nominal radii of 4, 12, and 50 μm. The ISE for spherical nanoindentation on np-Au is found to depend on the indenter radius, implying that the hardness for spherical nanoindentation decreases as the indenter radius increases at the same representative strain. A nanomechanics model for spherical indentation on np-Au is developed by assuming that the total indentation work is consumed by the plastic collapse in two loading modes represented by normal and shear forces. We investigate the correlation of the ISEs for spherical and sharp (Berkovich) indentations in terms of strain hardening and indentation work.

Np-Au samples with a ligament size of 26 nm were prepared based on the authors' previous work [27]. $Au_{30}Ag_{70}$ precursor alloys were fabricated using pure Au and Ag pellets by melting. After homogenization at 800 °C for 72 h under N_2 environment, the precursor alloys were pressed into discs with a thickness of approximately 1 mm using a universal testing machine (Instron 5982), and both sides of the discs were gently polished using a diamond suspension with a particle size of 0.25 μm. To release possible internal stress in precursor alloys induced by mechanical pressing and polishing, the precursor alloy discs were annealed in a tube furnace in a N_2 environment at 800 °C for 24 h. Nanoporosity was generated by free-corrosion dealloying in a 70% HNO_3 solution for 72 h at room temperature. Ligament sizes were measured by averaging the neck diameters at the centers of ligament connects, which are possibly the thinnest parts in the scanning electron microscope images.

Spherical nanoindentations were created using diamond spheroconical indenters with nominal tip radii of 4, 12, and 50 μm. We measured the effective radius, *R*, and the effective indentation depth of each spherical indenter by observing the side views using an optical microscope; the radii were 3.68 (±0.07) μm for the 4 μm nominal radius, 11.42 (±0.11) μm for the 12 μm nominal radius, and 54.99 (±0.39) μm for the 50 μm nominal radius. These effective radius values were used as the indenter radius, *R*. The effective indentation depth was the maximum height from the tip depth at which the indenter geometry was described by one value of the effective radius (Fig. 1(a)). The maximum indentation depths were less than this effective indentation depth. Spherical nanoindentations were created using the XP module of a G200 nanoindenter (Keysight) with a maximum load capacity of 500 mN in the CSM mode at an indentation strain rate of 0.05 s^{-1}.

The typical spherical indentation force–depth curves for np-Au are presented in Fig. 1. Fig. 2 shows the hardness as a function of the contact radius, *a*, when $a/R = 0.142$, where *R* is the indenter radius. $a/R = 0.142$ corresponds to the compressive yield strain, which is discussed in detail below. The hardness and the contact radius were calculated by the Oliver–Pharr method [28]. Fig. 2 shows that the hardness increases as the contact radius decreases; this behavior is similar to the ISE for spherical indentation of solid materials [4]. The hardness values in Fig. 2 were averaged from at least 15 reproducible indentation force–depth curves.

To analyze the ISE for spherical nanoindentation on np-Au, we developed a nanomechanics model based on the authors' previous work [27]. As shown in Fig. 3(a), from the indenter view, the spherical

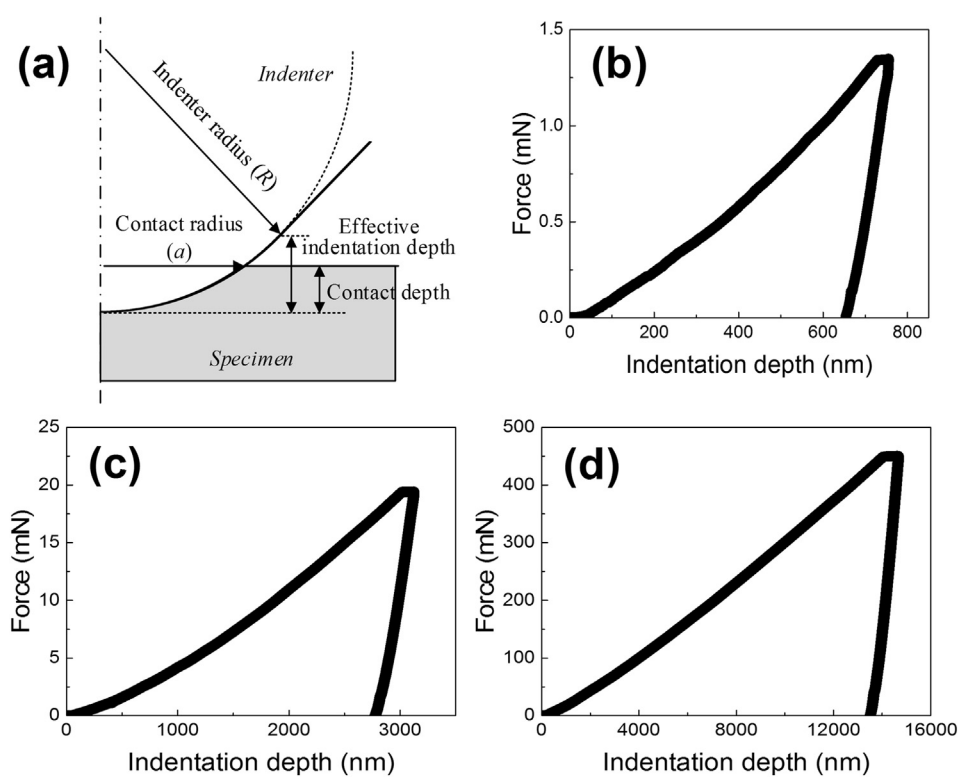

Fig. 1. (a) Schematic diagram of contact morphology, and typical nanoindentation force–depth curves for nominal indenter tip radii of (b) 4, (c) 12, and (d) 50 μm.